IEEE Trans. Information Forensics and Security, 2014

Efficient and Accurate at-a-distance Iris Recognition Using Geometric Key based Iris Encoding

Chun-Wei Tan, Ajay Kumar

Abstract—Accurate iris recognition from the distantly acquired face or eye images under less constrained environments require development of specialized strategies which can accommodate for significant image variations (e.g. scale, rotation, translation) and influence from multiple noise sources. A set of coordinate-pairs, which is referred to as *geometric key* in this paper is randomly generated and exclusively assigned to each subject enrolled into the system. Such geometric key uniquely defines the way how the iris features are encoded from the localized iris region pixels. Such iris encoding scheme involves computationally efficient and fast comparison operation on the locally assembled image patches using the locations defined by the geometric key. The image patches involved in such operation can be more tolerant to the noise. Scale and rotation changes in the localized iris region can be well accommodated by using the transformed geometric key. The binarized encoding of such local iris features still allows efficient computation of their similarity using Hamming distance. The superiority of the proposed iris encoding and matching strategy is ascertained by providing comparison with several state-of-the-art iris encoding and matching algorithms on three publicly available databases: UBIRIS.v2, FRGC, CASIA.v4-distance, which suggests the average improvements of 36.3%, 32.7% and 29.6% in equal error rates, respectively, as compared to several competing approaches.

I. INTRODUCTION

Automated iris recognition has emerged as one of the most promising biometrics technologies to provide reliable human identification. Almost all the existing commercial iris recognition systems acquire iris images using near infrared (NIR) imaging within short distance (typically between one to three feet) and under constrained environment. In other words, significant cooperation is expected from the users to provide their eye images while staring at imaging devices under such constrained environment. Such imaging can generally achieve remarkable

matching accuracy as iris texture is more clearly preserved in such high quality iris images acquired using NIR imaging under the constrained setup. The superiority of the NIR-based iris recognition technologies has been practically engaged in very large scale applications, such as in *Aadhar* project [8] to identify millions of citizens, or in border-crossing control system in UAE [9].

Recent advancement in the iris recognition technologies involves acquisition of the iris images *at-a-distance* and under *less constrained* environments using visible illumination imaging [10]-[12], [43]. Such systems are essentially desirable in meeting the increasingly demand for forensic and high security surveillance applications, for example, in providing critical early warning support to thwart for terrorism related threats [13]-[15]. The iris databases such as [11] and [12] are the attempts to acquire iris images at-a-distance and under less constrained environments using visible illumination in order to overcome several limitations of the existing commercial iris recognition system which are based on the NIR illumination. Such databases have been made available in the public domain with the endeavor to encourage further research in the development of new iris recognition technologies which can be more practical for forensic and surveillance applications.

(a) (b)

Figure 1: Sample iris/eye images acquired under (a) constrained environment using NIR illumination, (b) less constrained environment using visible illumination.

The iris images recovered from the distantly acquired face images, especially under less constrained imaging environments and/or under visible illumination, are usually noisier as compared to those images acquired from close distances under NIR illumination, as also shown from image samples in Fig. 1. These images are usually influenced by multiple sources of noise, such as motion/defocus blur, occlusions from eyelashes, hair and eyeglasses, reflections, off-angle and partial eye images. Therefore, development of *accurate* iris recognition techniques which can be more tolerant to noise is highly desirable. There have been some promising efforts to develop more accurate iris segmentation approaches for noisy iris/eye images acquired using

visible imaging [11], [13]-[22]. However, only very limited research efforts are dedicated in development of specialized iris encoding and matching algorithms which can accommodate imaging variations in the segmented iris images, with notable exceptions like those reported in [23]-[25] from NICE.II contest. The NICE.II was an open competition with the focus specifically on iris encoding and matching algorithms for noisy iris images acquired at-a-distance and under less constrained environments using visible illumination. Table 1 summarizes the best three winning algorithms from the NICE.II contest.

Table 1: Ranking of the best three iris encoding and matching approaches from NICE.II contest

Ranking	**Ref.**	**Methodology**	**Decidability Index**	**Iris Segmentation**
1	[26]	using multiple features computed from iris and periocular	2.5748	Manual
2	[27]	Adaboost is trained to select discriminative Gabor-based features	1.8213	Manual
3	[28]	fusion of existing iris/periocular encoding techniques	1.7786	Manual
This paper		exploits iris features from localized and global normalized iris image regions.	2.0774	Fully automated

Apparently, the best of the iris encoding and matching algorithm reported in [26] adopts a multimodal strategy which employs multiple pieces of information from the iris, periocular, color distribution, *etc*., and the performance improvement resulting from such by using such multimodal strategy is quite intuitive but encouraging. Therefore, our primary objective in this paper has been to develop an efficient and accurate iris encoding and matching strategy which *only* uses the iris features to provide more accurate iris recognition capability for iris images acquired at-a-distance and under less constrained imaging environments.

A. Motivation and Our Work

Most of the existing iris encoding and matching algorithms such as those reported in [29]-[35] have been developed to work for the iris images acquired from constrained environment using NIR illumination. Such approaches may not be effective to recover iris features which are embedded in such degraded eye images influenced by large imaging variations, *e.g.*, scale, translation and rotational variations. For example, the method described in [29] attempts to

estimate the fragile (inconsistent) bits in the iris codes and excludes those inconsistent bits in computing the matching scores. Such strategy has shown to be promising for close distance or for conventional iris images but is not adequate to accommodate large imaging variations observed in visible illumination images acquired from at-a-distance. Ref. [30] presents the extended work of [29] by employing a weighting strategy to quantify each bit in the iris code such that consistent bits are assigned with higher values (toward one) while inconsistent bits are assigned with lower values (toward zero). Although such weighting strategy has shown to be more tolerant to noise, it experiences the limitations similar to as in the approach [29] to effectively encode the iris features which contain large image variations. In ref. [34], sparse representation framework is employed for the iris recognition which attempts to recover the iris features using the sparse coefficients estimated from the dictionary. However, the construction of the sparse dictionary for noisy iris images can be quite challenging as the sparse coefficients can be hard to be accurately estimated during the recovery process. Therefore the recognition performance is expected to be highly influenced from the dictionary constructed using noisy iris images.

Our primary objective in this work has been to develop an efficient iris encoding and matching strategy which only uses the iris features to provide more accurate personal identification capability for both the visible and NIR illumination iris images acquired at-a-distance. Such iris images are generally likely to be influenced from the multiple sources of noise and the imaging variations from less constrained environment. Therefore the effective algorithms required to encode such iris images must be robust to the noise and high intra-class variations. The proposed iris encoding and matching strategy benefits from the simultaneous exploitation of the textural information from both localized and global iris region pixels. The localized iris encoding strategy owes its strength in better accommodating for the imaging variations, while the global iris encoding strategy has its strength in effective encoding of less noisy iris region pixels. The combined strategy using both the localized and global iris matching can provide more accurate iris matching capability and therefore can be beneficial in making better decisions. In our proposed localized iris encoding scheme, geometrical information is utilized to provide efficient encoding from the local iris region pixels. A set of coordinate-pairs, which is referred to as *geometric key* in this paper, is randomly (pseudorandom) generated and exclusively assigned to each subject enrolled into the system. Such geometric key can be considered as unique

(personalized) to each of the subjects and it uniquely defines the way how the iris features are encoded from the localized regions. Such personalized strategy is expected to improve the *separability* between the inter-class and intra-class distributions and therefore the improvement in iris recognition performance can be expected. The localized iris features are encoded on the basis of the binary test at locations (coordinate-pair) as defined by the geometric key. In order to ensure high robustness to the noise, locally assembled image patches which are centered at the coordinate-pairs defined by the geometric key are involved in such binary test operations to encode the iris features. The scale and rotational changes in the localized iris region can be as well addressed by configuring the geometric key. Simple transformation operations are applied to the geometric key, rather than to the iris images, which can provide a more computationally efficient alternative to encode the iris features. The encoded localized iris features are represented in the binary form, which still allows the matching of iris templates to be done efficiently using the Hamming distance. The main contributions from this paper can be summarized as follows:

- Iris images acquired at-a-distance and under less constrained environments are often influenced from the multiple noise sources and the imaging variations. Therefore, this paper proposes a new approach to recover and match the iris features by incorporating the geometrical information from local region pixels, which is expected to be more effective in accommodating the influences from noise and imaging variations. The superiority of the proposed iris encoding and matching strategy is ascertained by providing comparison with several competing iris encoding and matching approaches on three publicly available databases: UBIRIS.v2, FRGC and CASIA.v4-distance, which suggest average percentage of the improvement of *36.3%*, *32.7%* and *29.6%* in the equal error rate respectively (see Section 3.3).
- Another key advantage of the proposed iris encoding approach is its computational simplicity. The binarized template size is expected to be smaller than several competing iris encoding and matching techniques in the literature (see Table 5), which can significantly improve the matching speed. The proposed iris encoding and matching strategy is shown to be effective for both the distantly acquired iris images under visible and NIR illumination.

The rest of this paper is organized as follows. The proposed iris encoding and matching strategy is described in Section 2. We provide the performance evaluation on the proposed approach, as well as the comparison with other competing iris encoding algorithms in the literature in Section 3. Finally the discussion and conclusion from this paper are presented in Section 4.

II. GEOMETRIC KEY IRIS ENCODING STRATEGY

The block diagram of the proposed iris matching strategy for the iris images acquired *at-a-distance* and under *less constrained conditions* is shown in Fig. 2. The proposed iris matching strategy comprises of a localized geometric key (GeoKey) encoding scheme and a global phase

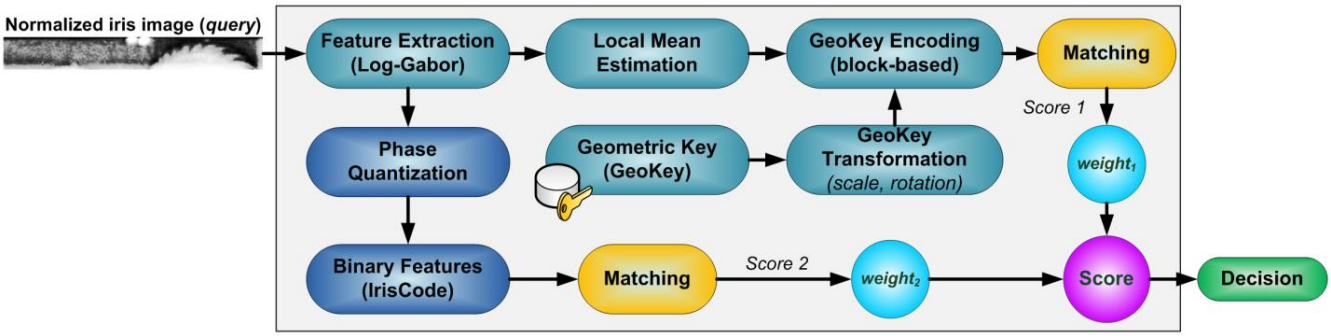

Figure 2: Block diagram of the proposed geometric key iris encoding scheme for iris images acquired at-a-distance and under less constrained conditions.

encoding scheme. The iris images acquired distantly and under less constrained imaging conditions are often influenced from severer level of imaging variations (e.g. *scale*, *rotation*) while the conventional iris encoding and matching techniques are designed to match iris images acquired from close distances in which iris features are more stable [29]-[35]. Therefore the feature encoding strategy shown in Fig. 2 emphasizes to accommodate inherent scale and rotational variations in the normalized or segmented iris images. The proposed iris feature encoding scheme incorporates the geometry information to encode iris texture details from the localized iris region pixels. Such geometrical information is determined by the GeoKey, which is a set of the coordinate-pairs exclusively assigned to each of the subjects enrolled into the system. The pseudorandom generated GeoKey is stored in the database together with the enrolled templates. Therefore, the GeoKey can be considered as a unique key which is personalized to each subject and uniquely defines the geometric location to encode the localized iris features. The proposed GeoKey encoding scheme works on the local region iris pixels and is therefore

expected to be more tolerant to the variations/noise as it can benefit from the intra-class features which are more likely to be preserved in the local iris regions. Furthermore, the GeoKey can be configured to account for scale and rotational changes in the localized iris region by applying simple transformation operations to the GeoKey. It is worth noting that such transformation operations are only applied to the GeoKey rather than to the iris images, which provides computationally efficient approach to encode the iris features. In order to exploit the global iris texture, the proposed scheme considers (Fig. 2) the global iris matchers such as Log-Gabor [35] to encode the global iris features. Such global iris matcher has its strength in matching less noisy iris region pixels and can be simultaneously computed using the localized GeoKey encoding scheme. We judiciously combine the information from both localized and the global iris matching scheme. This approach can accommodate higher intra-class imaging variations and allow us to make better decisions while identifying the query iris images.

A. Generating Geometric Key

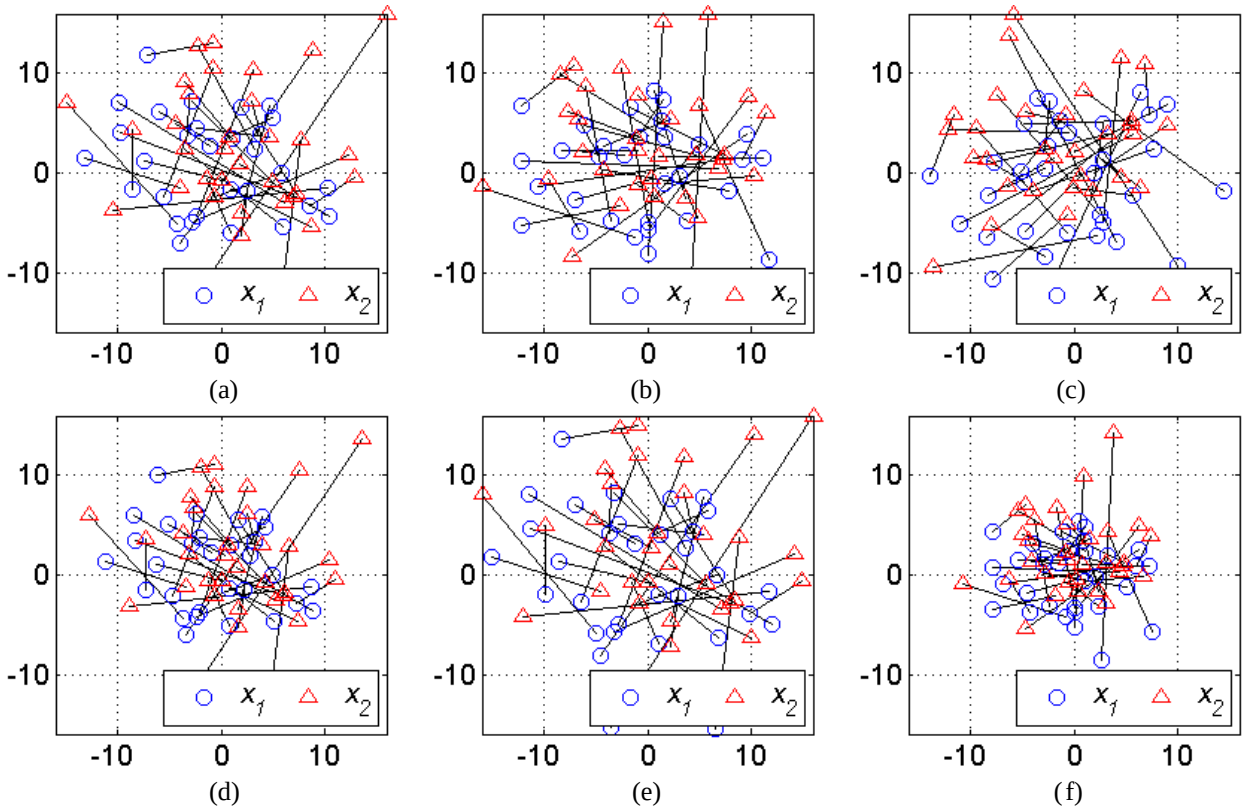

Figure 3: Examples of the GeoKey at different configurations ($B = 32; d = 32$). (a) original GeoKey, (b) rotation of (a) at $\theta = 30$-degree, (c) rotation of (a) at $\theta = 60$-degree, (d) scaled of (a) at $s = 0.85$, (e) scaled of (a) at $s = 1.15$, (f) scaled and rotation of (a) at $s = 0.65$ and $\theta = 30$-degree.

The geometric key K is a set of the coordinate-pairs of length d which define the locations in an image patch of size $B \times B$. Such geometric locations as defined by the GeoKey determine how the iris features are encoded from the localized iris region pixels. We employ the best out of the five configurations as discussed in [37] to generate the coordinate-pairs of length $d \leq B^2$, which is given as:

$$\boldsymbol{K} = \left\{(\boldsymbol{x_1}, \boldsymbol{x_2}) \sim \text{i. i. d. } G\left(0, \frac{1}{5}B\right)\right\}_{i=1,\ldots,d} \tag{1}$$

where $G(\cdot)$ is a Gaussian kernel with the mean equals to zero and the standard deviation equals to $1/5\,B$. Suppose there are N enrolled subjects in the system, a total of N GeoKeys $\{\boldsymbol{K}_d^1, \boldsymbol{K}_d^2, \ldots, \boldsymbol{K}_d^N\}$ will be generated and each of the enrolled subjects will be assigned with a GeoKey of length d.

The iris images acquired distantly and under less constrained conditions are often influenced from severer level of imaging variations such as scale and rotation in local region pixels. The proposed GeoKey iris encoding scheme can be configured to conveniently accommodate for such variations in the local region pixels. Unlike the work in [37], we apply the geometric transformations to the GeoKey rather than to the iris images using the Eq. (2) and (3), as given below:

$$\widetilde{\boldsymbol{K}}_s = \{SK_{i=1,\ldots,d}\};\ S = \begin{bmatrix} s & 0 \\ 0 & s \end{bmatrix} \tag{2}$$

$$\widetilde{\boldsymbol{K}}_\theta = \{RK_{i=1,\ldots,d}\};\ R = \begin{bmatrix} \cos\theta & \sin\theta \\ -\sin\theta & \cos\theta \end{bmatrix}, \tag{3}$$

where S and R represent the scaling matrix and rotation matrix [38], respectively (we use $s = \{0.85, 1, 1.15\}$ and $\theta = \{0°, 30°, 60°, 90°, 120°, 150°\}$ in the experiments). By applying the transformations on the GeoKey can be more computationally attractive as compared to the more demanding image transformation operations. The complexity of the transformations on the GeoKey depends on the key length of the GeoKey, which is typically much lower than the block size, *i.e.*, $d < B^2$ (see Table 3). Fig. 3 shows the examples of GeoKey configured to encode iris features at different orientations and scales.

B. Geometric Key Iris Encoding

Our iris encoding approach is inspired by the recent works in [36]-[37] which have shown to be

effective in accommodating the imaging variations from the local image regions. In this work, we exploit the iris features computed from the normalized iris images by performing the binary comparisons on the smoothed version of local windows $\mathbf{w}$ of size $S \times S$ using the locations as defined by the GeoKey, as illustrated in Fig. 4. The binary features f from an image patch can be computed as follows:

$$f(\mathbf{w}; \boldsymbol{x_1}, \boldsymbol{x_2} \in \boldsymbol{K}) = \begin{cases} 1 \; if \; L(\mathbf{w}, \boldsymbol{x_1}) < L(\mathbf{w}, \boldsymbol{x_2}) \\ 0 \; \text{otherwise}, \end{cases} \tag{4}$$

where $L(\mathbf{w}, \boldsymbol{x_1})$ denotes the filter responses from the Log-Gabor in the smoothed version of $\mathbf{w}$ at $\boldsymbol{x_1}$. The computation of the binary features is performed on the smoothed local windows in order to provide more reliable estimation of the iris features from the local iris regions. It is worth noting that the mean values of $\mathbf{w}$ can be efficiently approximated using the integral image

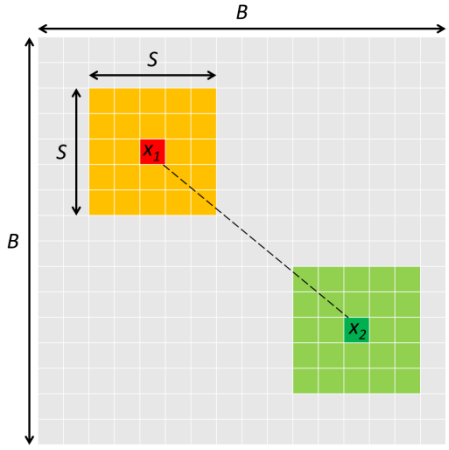

Figure 4: Illustration of the GeoKey iris encoding from an image patch of size $B \times B$. The binary test is performed on the local smoothing windows of size $S \times S$ centered at x_1 and x_2, respectively. Therefore, the x_1 and x_2 represent the average values of the filter responses computed from the respective local window w.

technique, which requires only three addition operations and a division operation. Therefore, the proposed GeoKey iris encoding scheme provides a different way from the conventional coarse phase quantization approaches [2], [35], which encodes the iris features by incorporating the geometry information. The encoded iris features are in the binary form and therefore can be efficiently matched using the Hamming distance, as given as follows:

$$HD^j = \frac{\left\| Code^j_{gallery} \oplus \mathbf{F}_{query}(\mathbf{W}, \boldsymbol{K}^j) \right\|}{p \times q}, \tag{5}$$

where $Code^j_{gallery} \in \mathbb{B}^{p \times q}$ denotes the binary gallery template of class j ;

$\mathbf{W} = [\mathbf{w}_1, \mathbf{w}_2, \ldots, \mathbf{w}_{p\times q}]$ represents the local windows. $\mathbf{F}_{query}(\mathbf{W}, \boldsymbol{K}^j) \in \mathbb{B}^{p\times q}$ represents the binary query template of size $p \times q$ encoded with the $\boldsymbol{K}^j$; '$\oplus$' denotes the XOR operator. In this paper, we employ an overlapping block strategy which extracts image patches from the normalized iris image at the interval $h = {}^{B}/_{2}$ in both horizontal and vertical directions. Therefore, the width p and height q of the template are depend on the width and height of the normalized iris image, block size $B \times B$, sliding interval h, and the key length d of GeoKey.

The proposed GeoKey iris encoding scheme is designed to provide localized encoding which can be more tolerant to the local region pixel variations such as rotation and scale changes[*]. However, the conventional coarse phase quantization approaches (global iris encoding) such as [2], [35], have its strength to encode the iris features in less noisy iris region pixels. Such coarse phase quantization approaches, *i.e.* Log-Gabor in this paper, can be conveniently acquired since that the feature extraction is a *common* procedure prior both the localized and global encoding schemes (see Fig. 2). Therefore, both the localized and global binarized iris features can be simultaneously computed without incurring expensive computation cost. The combined information from both the localized and the global iris matchers can provide more accurate matching accuracy (see Section 3.1) and therefore can benefit us to make better decisions.

III. EXPERIMENTS AND RESULTS

In this section, we detail on the experiments and present results from the rigorous experimentation on three publicly available databases: UBIRIS.v2 [11], [23], FRGC [40]-[41], and CASIA.v4-distance [42] to ascertain the performance from the proposed iris encoding and matching strategy. Three such databases are employed in the experiments due to their appropriateness to meet the research problem focused in this paper as the three databases were distantly acquired (ranging from 3-8 meters) under less constrained environments using either visible or NIR imaging. All the iris images employed in this paper use automated iris segmentation approach as described in [39], which has shown to be more accurate as it achieves superior segmentation accuracy for both the iris images acquired using visible and NIR imaging.

[*] Translation can be addressed by using the conventional circular bit shift operation during the matching phase.

A. Databases and Evaluation Protocols

All the experiments conducted in this work use subject of images from the three employed databases, as summarized in the Table 2. The segmented iris images from UBIRIS.v2, FRGC, and CASIA.v4-distance databases are respectively normalized to the sizes of 512×64, 256×32 and 512×64. The parameters as employed by the GeoKey encoding scheme and log-Gabor[†] encoding scheme are given in Table 3. All the parameters are obtained using a set of training images which are independent from the test images. For UBIRIS.v2 database, a subset of 1000 images from 171 subjects as released in [24] is employed in the experiments. The 96 images from the first 19 subjects are employed for estimating the log-Gabor parameters while the remaining segmented iris images are employed as test images for the performance evaluation. For FRGC database, a subset of high-resolution still images selected from session 2002-269 to 2002-317 of Fall2002 and Spring2003, which consists of a total of 1085 images from 149 subjects, is employed in the experiments. Such subset images are selected using the AdaBoost eye detector provided with OpenCV [45]. The images from the UBIRIS.v2 and the FRGC databases are in the RGB color space, we employ the luma-channel (Y) of the YCbCr after the color space conversion in the experiments. For CASIA.v4-distance database, the left eye images from the first 10 subjects are employed to compute the log-Gabor parameters. We use the first eight left eye images from the remaining 131 subjects as the independent test images for the performance evaluation. As for the performance evaluation, the test images from the employed databases are further divide into gallery and query images. In this paper, we employ the *first five images* (or at most[‡]) as the gallery dataset while the remaining images as the query dataset. The subset images which are randomly chosen from the gallery datasets are employed in estimating the parameters for the GeoKey iris encoding scheme (see Table 3) as described in Section 2.2.

Table 2: Numbers of images and subjects of the employed databases

Database	**UBIRIS.v2**	**FRGC**	**CASIA.v4-distance**
Imaging type	Visible	Visible	NIR
Number of images	864	1085	935
Number of subjects	151	149	131

[†] We use same protocol as reported in [15] and [39].

[‡] The number of images is varying for each distinct subject for UBIRIS.v2 and FRGC databases as some poor quality images were filtered out by the completely automated segmentation algorithm [39].

Table 3: Parameters employed by the proposed iris encoding scheme

Parameter / Database	GeoKey Encoding				Log-Gabor Encoding	
	B	***h***	***S***	***d***	***Wavelength***	***SigmaOnf***
UBIRIS.v2	32	16	7	96	59	0.32
FRGC	16	8	5	48	40	0.35
CASIA.v4-distance	32	16	7	128	20	0.25

B. Joint Local and Global Matching Scores

In this section, we report experimental results to achieve superior matching accuracy by simultaneously employ both the GeoKey encoded iris features and log-Gabor encoded iris features. The matching scores computed from both GeoKey encoding scheme and log-Gabor encoding scheme are combined at score level using weighted sum rule. Table 4 summarizes the weights employed to combine the matching scores from global and local iris features on different databases. Fig. 5 and 6 show the receiver operating characteristic (ROC) and cumulative match characteristic (CMC) plots from the three employed databases. These experimental results illustrate significantly improvement in the recognition performance especially for the verification problem (ROC), which suggest the superiority of the proposed matching strategy using joint information from both localized and global features. In summary, the combined scores from the localized and global iris features have been ascertained to achieve better discrimination than employing either global or localized iris features alone.

Table 4: Parameters used to combine global and local matching scores

Database	Weight		Rank-one Recognition Rate
	Global (Log-Gabor)	*Local (GeoKey)*	
UBIRIS.v2	0.23	0.77	46.4%
FRGC	0.40	0.60	48.1%
CASIA.v4-distance	0.43	0.57	92.9%

C. Performance Comparison

In order to further ascertain the recognition performance of the proposed iris encoding scheme for the distantly acquired iris images under less constrained environments, we have also provided comparison with several competing iris encoding approaches presented in the literatures: Fragile Bits [29], Personalized weight map (PWMap) [30], band-limited phase only correlation (BLPOC) [32], log-Gabor [39] and Sparse [34][§]. In this paper, we employ two of the commonly used

[§] The source code is publicly available at:
http://www.umiacs.umd.edu/~jsp/Research/SRRecognition/SparseRecognitionCancelability_PAMI2010.zip

performance metrics, *i.e.*, equal error rate (EER) and decidability index (*d*'), in the iris biometrics literatures [24], [26], [30] to show the recognition performance estimation from various approaches. The estimated recognition performance in the EER and *d*' from the various iris encoding approaches evaluated under the same protocol are summarized in Table 5. The ROC and CMC curves of various approaches are also provided in Fig. 7 and 8, respectively. The proposed iris encoding scheme has shown its superiority by outperforming the other state-of-the-art iris encoding approaches in both the EER and *d'*. The percentages of improvement for the proposed approach in terms of EER as compared to the other competing approaches are illustrated in Fig. 9. In summary, the proposed iris encoding approach achieves significant improvement over several state-of-the-art iris encoding techniques, which suggests percentage of improvements of *36.3%*, *32.7%* and *29.6%* on UBIRIS.v2, FRGC and CASIA.v4-distance databases, respectively.

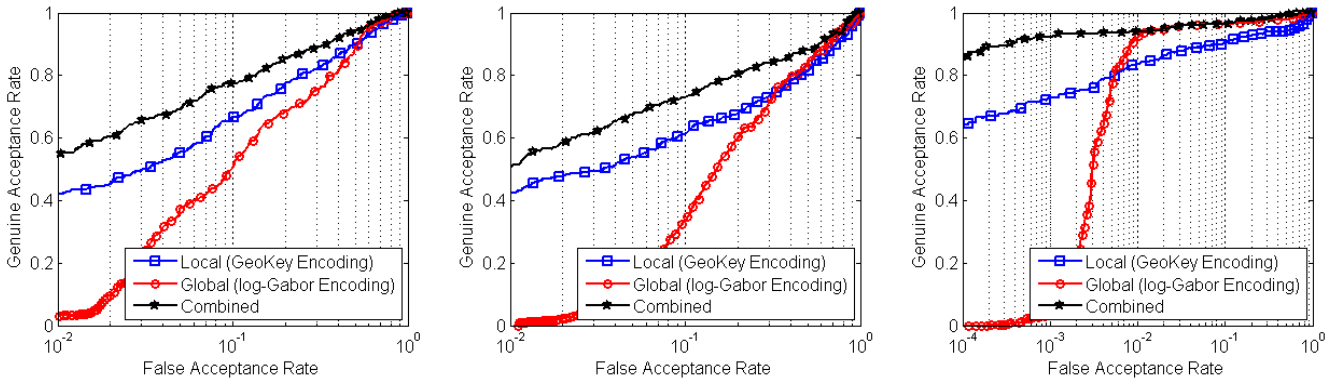

(a) (b) (c)

Figure 5: Receiver operating characteristics from the proposed approach on (a) UBIRIS.v2, (b) FRGC, (c) CASIA.v4-distance database.

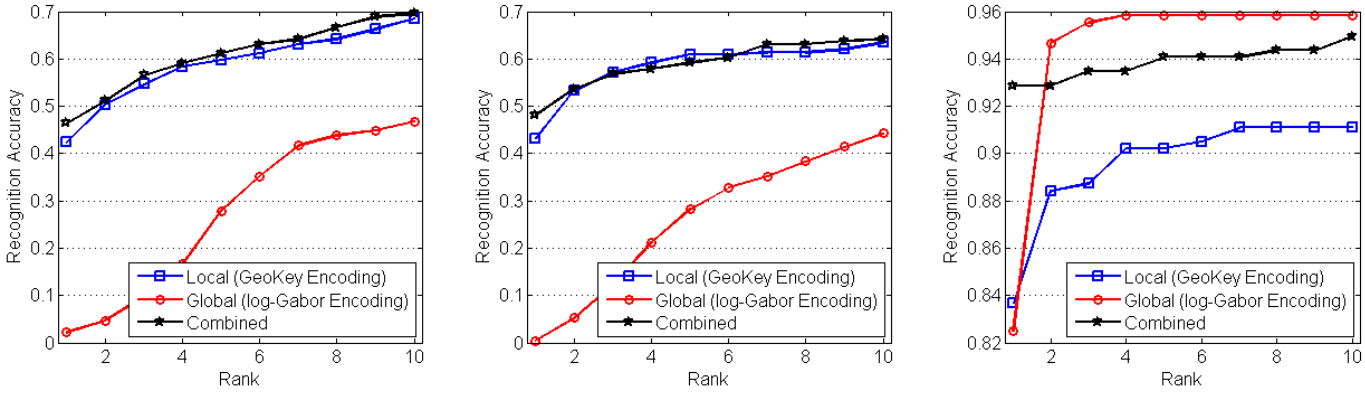

(a) (b) (c)

Figure 6: Cumulative match characteristics from the proposed approach on the (a) UBIRIS.v2, (b) FRGC, (c) CASIA.v4-distance database.

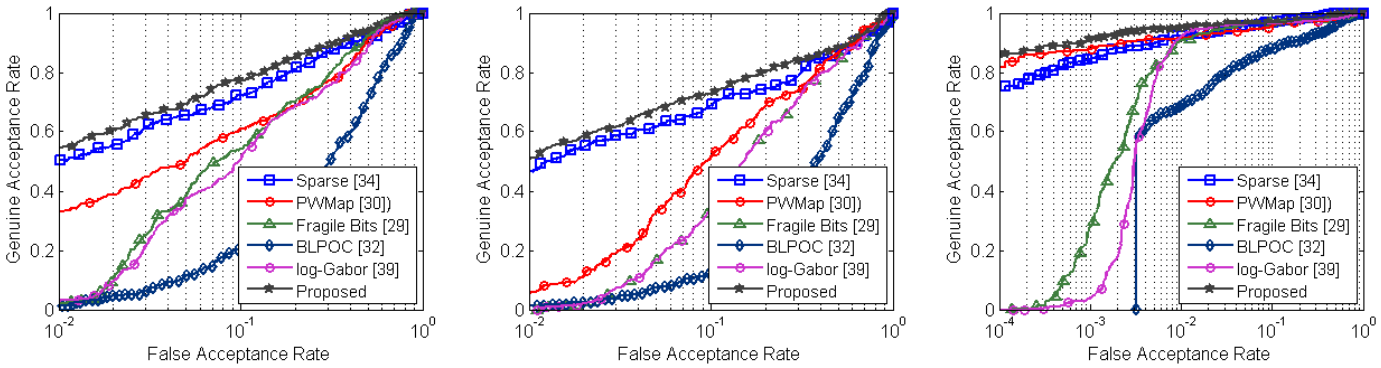

(a) (b) (c)

Fig. 7: Receiver operating characteristics from competing approaches using (a) UBIRIS.v2, (b) FRGC, (c) CASIA.v4-distance database.

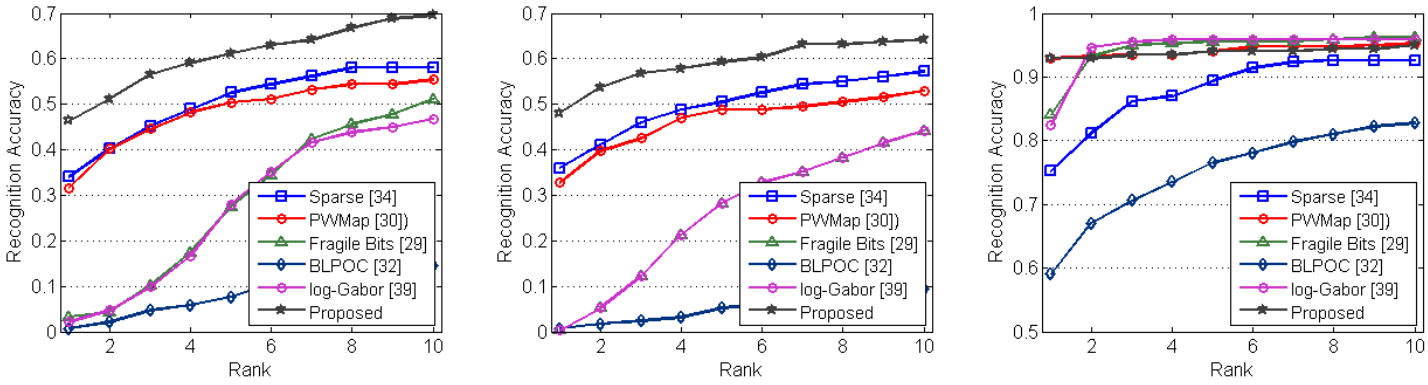

(a) (b) (c)

Figure 8: Cumulative match characteristics from competing approaches using (a) UBIRIS.v2, (b) FRGC, (c) CASIA.v4-distance database.

Table 5: The equal error rate and decidability index obtained by the different approaches from the three employed databases

	UBIRIS.v2		**FRGC**		**CASIA.v4-distance**	
Method	**Equal Error Rate**	**Decidability Index**	**Equal Error Rate**	**Decidability Index**	**Equal Error Rate**	**Decidability Index**
Sparse [34]	0.1922	1.5842	0.2397	1.4298	0.0445	3.4345
PWMap [30]	0.2608	1.3700	0.2681	1.1448	0.0564	3.4170
Fragile Bits [29]	0.2534	1.0923	0.2961	0.8284	0.0418	3.3054
BLPOC [32]	0.4022	0.4528	0.4396	0.2773	0.1136	2.6748
Log-Gabor [39]	0.2745	0.9266	0.2960	0.8280	0.0385	3.1525
This paper	**0.1667**	**2.0774**	**0.1987**	**1.7166**	**0.0356**	**5.3243**

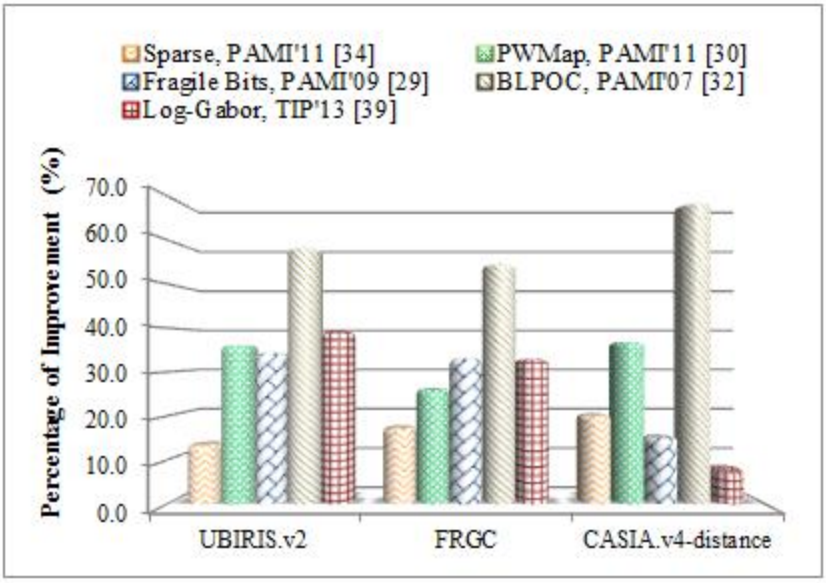

Figure 9: Expected improvement in equal error rate as compared to the competing approaches in literatures.

IV. DISCUSSION AND CONCLUSIONS

This paper has investigated a promising iris encoding and matching strategy for the noisy iris images acquired at-a-distance and under less constrained environments using both visible and NIR imaging. The approach presented in this paper simultaneously exploits the iris features computed from both the localized iris regions and global feature representations. The localized iris encoding scheme owes its strength to better accommodate for imaging variations, while the global iris encoding scheme can be more effective in less noisy iris region pixels. The superiority of the proposed iris encoding and matching strategy has been ascertained by providing comparison with several competing iris encoding and matching algorithms in the literature using the same protocol on three publicly available databases: UBIRIS.v2, FRGC, CASIA.v4-distance, which suggest improvements of *36.3%*, *32.7%* and *29.6%* in equal error rates, respectively. It is worth noting that such encouraging recognition performance is achieved by solely employing the iris information. Our approach does not consider the multimodal strategy as presented in [26], [28] as such performance improvement is quite intuitive/expected. Furthermore the algorithms in [26], [28] were evaluated using noise-free iris images[**], which may not sufficient to provide accurate estimation of the actual performance for a deployable iris recognition system. Another attractiveness of the proposed iris encoding and matching strategy is its efficiency in both

[**] The iris images were manually segmented and have least/negligible influence from the segmentation errors.

computation and memory requirements. The iris matching for both localized and global binarized iris features can be computed in very efficient way using the Hamming distance [1]-[3]. Table 6 summarizes the requirement of the memory storage[††] by the best three performing iris encoding and matching algorithms from our experiments on the three employed databases, which suggests that much lower memory storage is required by the proposed iris encoding and matching strategy. Table 7 summarizes the average computational times required to encode and match one iris template as compared to the best performing algorithm, *i.e.* Sparse [34]. All the implementations were done in Matlab and executed on Intel i5 2.5GHz processor with 4GB RAM in Microsoft Windows 7 environment. This table suggests that the matching of the GeoKey encoded binarized templates can be 0.7s faster, on an average, as compared to those using the templates from the Sparse representation based method in [34]. This increase in matching speed can be largely attributed to the resulting binarized templates which are compact (table 6) in size. However, the average computational time required to perform the GeoKey encoding is more demanding as it involves more localized complex operations (see Section II). The approach in reference [34] requires only the Log-Gabor encoding operations and therefore it is expected to consume less time for the computations. In summary, the iris encoding and matching strategy as investigated in this paper has achieved encouraging matching accuracy, especially for the visible-light iris images. However, further research efforts are still required in this area in order to make any inroads for the commercial applications, *e.g.* forensic and surveillance applications. Further work should also be directed to improving the recognition accuracy for the distantly acquired iris images. One of the possible solutions is to incorporate the occlusion masks[‡‡] into the GeoKey iris encoding scheme. Conventionally, the occlusion masks are designed to work and be used for the global iris encoding schemes in order to prevent non-iris pixels from degrading the recognition performance [2]-[3]. The proposed GeoKey encoding scheme however involves localized operations and therefore the development of new techniques to enable incorporation of the occlusion masks is highly desirable. Another strategy worthy of investigation is to incorporate different GeoKey generation functions which can be optimized for each of the subjects during their enrollment. The limitations of this work and the possible

[††] Template sizes are based on the sizes of the normalized iris images as employed in this paper.
[‡‡] Occlusion mask can be obtained automatically during iris segmentation stage.

improvements from more localized and user-specific strategies are to be pursued in our future work.

Table 6: Requirement of memory storage by the best three performing algorithms from our experiments on the three employed databases

Method \ Database	Memory Requirement Per Iris Template / Weight Map (bytes)		
	UBIRIS.v2	FRGC	CASIA.v4-distance
Sparse [34]	262144	65536	262144
PWMap [30]	4096 + 32768	1024 + 8192	4096 + 32768
Fragile Bits [29]	4096 + 4096	1024 + 1024	4096 + 4096
GeoKey + Log-Gabor	192 + 4096	96 + 1024	256 + 4096

Table 7: Average computation times required to encode and match one iris template

Method	Average Execution Time (second)	
	Encoding	Matching
Sparse [34]	0.0029	0.7887
GeoKey	1.4084	0.0878

REFERENCES

[1] K. Bowyer, K. Hollingsworth and P. Flynn, "Image understanding for iris biometrics: A survey," *Image & Vision Comput.*, vol. 110, no. 2, 2008.

[2] J. Daugman, "How iris recognition works," *IEEE Trans. Circuits Syst. Video Technol.*, vol. 14, no. 1, pp. 21-30, 2004.

[3] J. Daugman, "New methods in iris recognition," *IEEE Trans. Syst. Man Cybern. Part B Cybern.*, vol. 37, no. 5, p. 1167–1175, 2007.

[4] R. Wildes, "Iris Recognition: An emerging biometric technology," *Proc. Of IEEE,* vol. 85, no. 9, pp. 1348-1363, 1997.

[5] Z. He, T. Tan, Z. Sun and X. Qiu, "Toward accurate and fast iris segmentation for iris biometrics," *IEEE Trans. Pattern Anal. Mach. Intell.*, vol. 31, no. 9, p. 1670–1684, 2009.

[6] A. Kumar and A. Passi, "Comparison and combination of iris matchers for reliable personal authentication," *Pattern Recognit.*, vol. 43, no. 3, 2010.

[7] S. Shah and A. Ross, "Iris segmentation using geodesic active contours," *IEEE Trans. Inf. Forensics Secur.*, vol. 4, pp. 824-836, 2009.

[8] *Role of biometric technology in Aadhaar enrollments, UID Authority of India*, Jan 2012. Available online: http://uidai.gov.in/images/FrontPageUpdates/role_of_biometric_technology_in_aadhaar_jan21_2012.pdf.

[9] J. Daugman, "Iris recognition at airports and border crossings," pp. 819-825, in *Encyclopedia of Biometrics*, Springer, 2009.

[10] J. Matey, O. Naroditsky, K. Hanna, R. Kolczynski, D. LoIacono, S. Mangru, M. Tinker, T. Zappia and W. Zhao, "Iris on the move: acquisition of images for iris recognition in less constrained environments," *Proc. IEEE,* vol. 94, no. 11, pp. 1936-1947, 2006.

[11] H. Proenca and L. Alexandre, "UBIRIS: A noisy iris image database," *Proc. ICIAP 2005, Intern. Conf. Image Analysis and Processing,* 2005.

[12] H. Proenca, S. Filipe, R. Santos, J. Oliveira and L. Alexandre, "The UBIRIS.v2: A database of visible wavelength images captured on the move and at-a-distance," *IEEE Trans. Pattern Anal. Mach. Intell.*, vol. 32, no. 8, pp. 1529-1535, 2010.

[13] H. Proenca, "Iris recognition: on the segmentation of degraded images acquired in the visible wavelength," *IEEE Trans. Pattern Anal. Mach. Intell.*, vol. 32, no. 8, pp. 1502-1516, 2010.

[14] C.-W. Tan and A. Kumar, "Automated segmentation of iris images using visible wavelength face images," *Proc. CVPR 2011,* 2011.

[15] C.-W. Tan and A. Kumar, "A unified framework for automated iris segmentation using distantly acquired face images," *IEEE Trans. Image Process.*, vol. 21, no. 9, pp. 4068-4079, 2012.
[16] T. Tan, Z. He and Z. Sun, "Efficient and robust segmentation of noisy iris images for non-cooperative iris recognition," *Image Vision Comput.*, vol. 28, no. 2, pp. 223-230, 2010.
[17] D. S. Jeong, J. W. Hwang, B. J. Kang, K. R. Park, C. S. Won, D.-K. Park and J. Kim, "A new iris segmentation method for non-ideal iris images," *Image Vision Comput.*, vol. 28, no. 2, pp. 254-260, 2010.
[18] P. Li, X. Liu, L. Xiao and Q. Song, "Robust and accurate iris segmentation in very noisy iris images," *Image Vision Comput.*, vol. 28, no. 2, pp. 246-253, 2010.
[19] W. Sankowski, K. Grabowski, M. Napieralska, M. Zubert and A. Napieralski, "Reliable algorithm for iris segmentation in eye image," *Image & Vision Comput.*, vol. 28, no. 2, pp. 231-237, 2010.
[20] R. D. Labati and F. Scotti, "Noisy iris segmentation with boundary regularization and reflections removal," *Image Vision Comput.*, vol. 28, no. 2, p. 270–277, 2010.
[21] Y. Chen, M. Adjouadi, C. Han, J. Wang, A. Barreto, N. Rishe and J. Andrian, "A highly accurate and computationally efficient approach for unconstrained iris segmentation," *Image Vision Comput.*, vol.28, 2010.
[22] M. A. Luengo-Oroz, E. Faure and J. Angulo, "Robust iris segmentation on uncalibrated noisy images using mathematical morphology," *Image Vision Comput.*, vol. 28, no. 2, p. 278–284, 2010.
[23] NICE:II - Noisy Iris Challenge Evaluation, Part II., [Online]. Available: http://nice2.di.ubi.pt/.
[24] H. Proenca and L. Alexandre, "Toward covert iris biometric recognition: experimental results from the NICE contests," *IEEE Trans. Inf. Forensics Secur.*, vol. 7, pp. 798-808, 2012.
[25] K. Bowyer, "The results of the NICE.II iris biometrics competition," *Pattern Recognit. Lett.*, vol. 33, no. 8, pp. 965-969, 2012.
[26] T. Tan, X. Zhang, Z. Sun and H. Zhang, "Noisy iris image matching by using multiple cues," *Pattern Recognit. Lett.*, vol. 33, pp.979-977, 2012.
[27] Q. Wang, X. Zhang, M. Li, X. Dong, Q. Zhou and Y. Yin, "Adaboost and multi-orientation 2D Gabor-based noisy iris recognition," *Pattern Recognit. Lett.*, vol. 33, no. 8, pp. 978-983, 2012.
[28] G. Santos and E. Hoyle, "A fusion approach to unconstrained iris recognition," *Pattern Recognit. Lett.*, vol. 33, no.8, pp. 984-990, 2012.
[29] K. Hollingsworth, K. Bowyer and P.J. Flynn, "The best bits in an iris code," *IEEE Trans. Pattern Anal. Mach. Intell.*, vol.31, 2009.
[30] W. Dong , Z. Sun and T. Tan, "Iris matching based on personalized weight map," *IEEE Trans. Pattern Anal. Mach. Intell*, vol. 33, no. 9, pp. 1744-1757, 2011.
[31] D. Monro, S. Rakshit and D. Zhang, "DCT-based iris recognition," *IEEE Trans. Pattern Anal. Mach. Intell.*, vol. 29, pp. 586-595, 2007.
[32] K. Miyazawa, K. Ito, T. Aoki, K. Kobayashi and H. Nakajima, "An effective approach for iris recognition using phase-based image matching," *IEEE Trans. Pattern Anal. Mach. Intell.*, vol. 30, 2007.
[33] Z. Sun and T. Tan, "Ordinal measures for iris recognition," *IEEE Trans. Pattern Anal. Mach. Intell.*, vol. 31, no. 12, pp. 2211-2226, 2009.
[34] J. Pillai, V. Patel, R. Chellappa and N. Ratha, "Secure and robust iris recognition using random projections and sparse representations," *IEEE Trans. Pattern Anal. Mach. Intell*, vol. 33, pp. 1877-1893, 2011.
[35] L. Masek and P. Kovesi, "MATLAB source code for a biometric identification system based on iris patterns," The School of Computer Science and Software Engineering, The University of Western Australia, 2003. [Online]. Available: http://www.csse.uwa.edu.au/~pk/studentprojects/libor/.
[36] M. Ozuysal, M. Calonder, V. Lepetit and P. Fua, "Fast Keypoint Recognition Using Random Ferns," *IEEE Trans. Pattern Anal. Mach. Intell*, vol. 32, no. 3, pp. 448-461, 2010.
[37] M. Calonder, V. Lepetit, M. Ozuysal, T. Trzcinski, C. Strecha and P. Fua, "BRIEF: Computing a Local Binary Descriptor Very Fast," *IEEE Trans. Pattern Anal. Mach. Intell*, vol. 34, no. 7, pp. 1281-1298, 2012.
[38] K. Jänich, *Linear algebra*, New York: Springer-Verlag, 1994.
[39] C.-W Tan and A. Kumar, "Towards online iris and periocular recognition under relaxed imaging constraints," *IEEE Trans. Image Process.*, vol. 22, no. 10, pp. 3751-3765, 2013.
[40] "Face Recognition Grand Challenge – Overview.," [Online]. Available: http://www.nist.gov/itl/iad/ig/frgc.cfm.
[41] P. Phillips, P. Flynn, T. Scruggs, K. Bowyer, J. Chang, K. Hoffman, J. Marques, J. Min and W.Worek, "Overview of the face recognition grand challenge," *Proc. CVPR 2005*, 2005.
[42] "CASIA.v4 database.," [Online]. Available: http://biometrics.idealtest.org/dbDetailForUser.do?id=4.

[43] M. Vatsa, R. Singh, A. Ross and A. Noore, "Quality-based Fusion for Multichannel Iris Recognition," *Proc. ICPR*, (Istanbul, Turkey), 2010.
[44] A. Kong, D. Zhang and M. Kamel, "An analysis of IrisCode," *IEEE Trans. Image Process.*, vol. 19, No. 2, pp. 522-532, 2010.
[45] OpenCV. [Online]. Available: http://opencv.org/